

REDUCED MEMORY MODELING AND EQUALIZATION OF SECOND ORDER FIR VOLTERRA CHANNELS IN NON-COHERENT UWB SYSTEMS

Jac Romme[†] and Klaus Witrisal[‡]

[†]IMST GmbH, Carl-Friedrich-Gauss Str. 2, D-47475, Kamp-Lintfort, Germany, romme@imst.de

[‡]Graz University of Technology, Inffeldgasse 12, A-8010 Graz, Austria, witrisal@tugraz.at

ABSTRACT

This paper investigates a combination of two approaches to obtain high data-rate UWB communication over multipath radio channels, using low complexity, non-coherent receivers. The first approach targets to equalize the occurring *non-linear* ISI using trellis-based equalization, while the second approach aims to reduce or even avoid ISI by dividing the spectral resources into (a few) sub-bands. Combination of both concepts allows for a complexity trade-off between equalizer and RF front-end. Firstly, a reduced-memory data model will be introduced for the non-linear sub-band channels, optimal in the sense of the MMSE criterion. This model is used to study the relationship between equalizer complexity and performance. The second part of the paper investigates the performance of the complete system, before and after forward error control. The system uses QPSK-TR signaling, but the key concepts are applicable to other non-coherent UWB systems as well.

1. INTRODUCTION

In the early days, UWB technology was promised to provide high data-rate communication to the mass market at very low-cost, while consuming little (battery) power. Due to the richness of the multipath channel combined with the high time-resolution of UWB signals, it quickly became apparent that linear, coherent receiver concepts, known from narrowband systems, become very complex in the UWB case. Having this in mind, part of the UWB community began investigating simple, non-linear, non-coherent receiver architectures. Especially, energy detecting receivers (EDR) [1, 2] and autocorrelation receivers (AcR) [3, 4, 5] became object of investigation. From a mathematical point of view, both receiver types are rather similar. An EDR can namely be seen as an AcR matched at lag zero. As a result, much of the insight obtained for one receiver type can be ported to the other.

In this work, an AcR-based system will be investigated on its ability to provide for indoor, high data-rate UWB communication. As signaling scheme, QPSK transmitted-reference (TR) modulation will be used, which will be demodulated using a fractionally sampled, complex-valued (CV) AcR [6]. It has been shown that the complete communication scheme from the transmitted QPSK-TR symbols until the CV samples generated by the AcR can be modeled using a second-order, finite-impulse-response (FIR) Volterra model.

To support high data-rates, the receiver must be able to equalize the FIR Volterra channel [7]. In this paper, the performance of trellis-based equalization is investigated with respect to its complexity. Alternatively, the spectral resource

can be divided into sub-bands [2]. In each sub-band, the data-rate will be relatively low, such that less ISI will occur, while the accumulated data-rate can still be high. Both concepts are applied to the system architecture with the aim to provide for a high rate data communication, while limiting the overall system complexity.

In [8], a decision feedback equalizer (DFE) is investigated for an EDR, which is sub-optimal by nature. A DFE namely forces a receiver to take a decision on the bit value, before receiving all the related energy. Furthermore, it neglects the presence of a Volterra channel and assumes a linear channel. On the other hand, it has a low complexity and is therefore appropriate for certain applications.

In Sec. 2, the signaling scheme and the system model derived in [6] are briefly reviewed and adapted to the objectives of this paper. It is explained how the system model can be seen as a finite state machine. In Sec. 3, a sub-optimal, reduced memory, FIR Volterra channel is derived, which is optimal in the sense of the MMSE criterion. An equalizer using this reduced memory data model (RMDS) will have less complexity at the cost of performance. In Sec. 4, the concept of multi-band communication is applied to QPSK-TR to limit the ISI. Simulation results are analyzed in Sec. 5, to study the trade-off between the amount of sub-bands, equalizer complexity and performance, with and without forward error control. Conclusions are drawn in Sec. 6.

2. SIGNALING SCHEME AND SYSTEM MODELS

2.1 Signaling Scheme and system model

In a basic transmitted-reference (TR) UWB signaling scheme, a symbol waveform consists of two identically-shaped pulses $p(t)$, transmitted D seconds apart. The first pulse remains un-modulated, while the second is modulated by data. By selecting D small compared to the coherence time of the channel, both pulses are distorted equally by the channel, such that the AcR can use the first pulse as reference for the demodulation of the second. In this work, the reference pulse is allowed to be modulated as well, for instance to avoid spikes in the power spectral density of the transmit signal. The modulation applied to the reference and data-carrying pulses will be denoted by $\tilde{b}[n]$ and $b[n]$, respectively. The baseband equivalent of the transmitted (TX) signal can be written as

$$s(t) = \sum_n \tilde{b}[n]p(t, nT_s) + b[n]p(t, D + nT_s) \quad (1)$$

where $p(t, \tau)$ is the baseband equivalent of $p(t - \tau)$. Note that both $\tilde{b}[n]$ and $b[n]$ can be complex valued (CV), since a baseband equivalent notation is used. An on/off-keying sig-

nal can be expressed by (1), if D is chosen equal to zero, $\tilde{b}[n]$ is kept unmodulated to one, and $b[n]$ is BPSK modulated.

In [6], a fractionally-sampled, CV AcR was proposed for the demodulation of TR signals. This receiver takes L CV samples for each transmitted symbol. In the same work, the relation between TX symbols and the samples was modeled using a single-input, multiple-output (SIMO), FIR Volterra system, where the number of outputs equals L .

Without loss of generality, we assume each sample to be influenced by $M + 1$ data symbols. Thus, the value of the sample corresponding to the n -th symbol at the α -th output is denoted by

$$u[n, \alpha] = \mathbf{d}[n]^H \mathbf{K}_\alpha \mathbf{d}[n] + \eta[n, \alpha] \quad (2)$$

where \mathbf{K}_α and $\eta[n, \alpha]$ denote a second-order Volterra kernel and noise, respectively. The noise variance is output specific noise and will be denoted by $\sigma_{\eta, \alpha}^2$. The symbol vector $\mathbf{d}[n]$ is defined as

$$\mathbf{d}[n] = [\tilde{b}[n-M] \dots \tilde{b}[n] \quad b[n-M] \dots b[n]]^T \quad (3)$$

2.2 Signal Model in Vector Notation

It is convenient to write the Volterra system in a vector notation, such that

$$u[n, \alpha] = \tilde{\mathbf{d}}[n]^H \mathbf{k}_\alpha + \eta[n, \alpha]. \quad (4)$$

Usually, the vectors $\tilde{\mathbf{d}}[n]$ and \mathbf{k}_α are defined to be equal to $\text{vec}(\mathbf{d}[n]\mathbf{d}[n]^H)$ and $\text{vec}(\mathbf{K}_\alpha)$, respectively, where the operator $\text{vec}(\mathbf{M})$ creates a column vector by stacking the columns of \mathbf{M} . However, the elements in $\text{vec}(\mathbf{d}[n]\mathbf{d}[n]^H)$ are potentially correlated. In this case, its non-central auto-covariance matrix, which is defined as

$$\mathbf{A} \triangleq \text{E} \left[\text{vec}(\mathbf{d}[n]\mathbf{d}[n]^H) \text{vec}(\mathbf{d}[n]\mathbf{d}[n]^H)^H \right], \quad (5)$$

will not be full-rank. In other words, the rank $N_k = \text{rank}(\mathbf{A})$ is less than $(2M+2)^2$. Hence, $\text{vec}(\mathbf{d}[n]\mathbf{d}[n]^H)$ will be driven by N_k uncorrelated variables. Assuming these variables to be gathered in $\tilde{\mathbf{d}}[n]$, a linear transformation matrix \mathbf{T} must exist, which fulfills the following two criteria:

$$\mathbf{T}\tilde{\mathbf{d}}[n] = \text{vec}(\mathbf{d}[n]\mathbf{d}[n]^H) \quad (6)$$

$$\text{E}[\tilde{\mathbf{d}}[n]\tilde{\mathbf{d}}[n]^H] = \mathbf{I}_{N_k, N_k}. \quad (7)$$

Assuming \mathbf{T} to be available, $\tilde{\mathbf{d}}[n]$ and \mathbf{k}_α can be obtained by

$$\tilde{\mathbf{d}}[n] = \mathbf{T}^\dagger \text{vec}(\mathbf{d}[n]\mathbf{d}[n]^H), \quad (8)$$

$$\mathbf{k}_\alpha = \mathbf{T}^H \text{vec}(\mathbf{K}_\alpha). \quad (9)$$

In the cases we considered, the composition of \mathbf{A} was rather simple, i.e. the elements of $\text{vec}(\mathbf{d}[n]\mathbf{d}[n]^H)$ are either fully or not correlated. This made the construction of the transformation matrix \mathbf{T} straight-forward and such that the elements in $\tilde{\mathbf{d}}[n]$ all appear one-to-one in $\text{vec}(\mathbf{d}[n]\mathbf{d}[n]^H)$. Note that one element in $\tilde{\mathbf{d}}[n]$ will have a constant value one for all possible realization of $\text{vec}(\mathbf{d}[n]\mathbf{d}[n]^H)$, which without loss of generality, is assumed to be the first element of $\tilde{\mathbf{d}}[n]$.

Alternatively, we noticed that the transformation matrix \mathbf{T} can also be obtained from an eigendecomposition $\mathbf{A} =$

$\mathbf{E}\mathbf{\Lambda}\mathbf{E}^H$, where \mathbf{E} is the unitary matrix of eigenvectors and $\mathbf{\Lambda}$ is a diagonal matrix of eigenvalues. The transformation matrix \mathbf{T} is then obtained from

$$\mathbf{T} = \mathbf{E}_{NZ} \sqrt{\mathbf{\Lambda}_{NZ}} \quad (10)$$

where the zero-eigenvalues and the corresponding eigenvectors are skipped, as denoted by the subscript NZ . It is unclear to us, whether this generally yields an appropriate mapping, or only in our context.

2.3 Signal Model seen as Finite State Machine

The modulation applied to both pulses has been kept general so far. In practice, $\log_2(N_s)$ (channel) bits will be communicated over the channel per symbol. Assuming these bits to be i.i.d. RVs in $\mathbb{B} = \{0, 1\}$, the symbols $s[n]$ will be i.i.d. RVs in $\{0, 1, \dots, N_s - 1\}$, with equal probability. The n -th symbol $s[n]$ determines the value of both $\tilde{b}[n]$ and $b[n]$. The mapping of $s[n]$ onto $\tilde{b}[n]$ and $b[n]$ is denoted by the functions $\tilde{g}(\cdot)$ and $g(\cdot)$, respectively. Hence, the vector $\mathbf{d}[n]$ can be written as

$$\mathbf{d}[n] = [\tilde{g}(s[n])^T \quad g(s[n])^T]^T \quad (11)$$

where $s[n] \triangleq [s[n-M] \dots s[n]]^T$ and $\tilde{g}(\cdot)$ and $g(\cdot)$ are defined to operate element-wise.

As any other FIR filter, the FIR Volterra system of (2) can be described using a tapped-delay-line. I.e. it can be seen as a finite state machine (FSM), such that

$$u[n, \alpha] = f_\alpha(s[n], S_t[n]) + \eta[n, \alpha] \quad (12)$$

where $S_t[n]$ denotes the current state and the total number of distinct states N_{S_t} equals N_s^M . In the absence of noise, the output depends on $s[n]$ and $S_t[n]$ only. Afterwards, the state is updated, where $S_t[n+1]$ depends only on $s[n]$ and $S_t[n]$. The function $f_\alpha(\cdot, \cdot)$ is specific for each output, but all outputs are driven by the same symbols.

3. REDUCED MEMORY DATA MODEL

It is well-known that FIR Volterra channels can be equalized using trellis-based algorithms, like a Viterbi or a Log-Map algorithm. These algorithms consider the channel as a FSM driven by the TX symbols and often assume the output(s) of the FSM to contain additive white Gaussian noise. Using knowledge on the structure of the channel FSM, both algorithms conduct a probabilistic computation to obtain the most likely transmitted sequence or symbol, respectively. In case of the Log-Map algorithm, the variance of the noise needs to be estimated as well.

The complexity of a trellis is proportional to the number of channel-states. I.e., it is exponentially proportional to the channel memory. As a result, trellis-based algorithms quickly become too complex for practical application, if they take the full channel memory into account. In this section, a reduced-memory data model (RMDM) is introduced, which mimics the behavior of the full data model (FDM), while using less memory. Using the RMDM, trellis-based algorithms can equalize the channel with less complexity at the cost of an increased sensitivity to noise. The RMDM will be shown to be optimal in the sense of the MMSE criterion.

The structure of the RMDM and the FDM are basically the same. Only the incoming symbols are delayed by m and

the memory N of the RMDM is less or equal to the FDM's memory M . In a vectorial notation, the output of the RMDM is defined as

$$\check{u}[n, \alpha] = \check{\mathbf{d}}[n-m]^H \check{\mathbf{k}}_\alpha + \check{\eta}[n, \alpha]. \quad (13)$$

where $\check{\mathbf{d}}[n]$ is of length N_r and related to a subset of $2N+2$ elements of the symbol vector $\mathbf{d}[n]$. A similar transformation as derived in Sec. 2.2 will relate $\text{vec}(\mathbf{d}[n]\mathbf{d}[n]^H)$ to $\check{\mathbf{d}}[n]$.

It is the challenge to find the optimal combination of kernels $\check{\mathbf{k}}_\alpha$ and a delay m , such that

$$[m, \check{\mathbf{k}}_\alpha] = \underset{x \in \mathbb{N}, \mathbf{k} \in \mathbb{C}^{N_r, 1}}{\text{argmin}} \left[\sum_{\alpha=1}^L \mathbb{E} \left[|\check{\mathbf{d}}[n]^H \mathbf{k}_\alpha - \check{\mathbf{d}}[n-x]^H \mathbf{k}|^2 \right] \right] \quad (14)$$

where \mathbb{N} and \mathbb{C} denote the sets of non-negative integers and complex numbers, respectively. To our knowledge, (14) can not be solved in closed form. Therefore, the MMSE solution for \mathbf{k}_α is derived for a single given output and delay x , denoted by $\check{\mathbf{k}}_\alpha^{(x)}$, such that

$$\check{\mathbf{k}}_\alpha^{(x)} = \underset{\mathbf{k} \in \mathbb{C}^{N_r, 1}}{\text{argmin}} \left[\mathbb{E} \left[|\check{\mathbf{d}}[n]^H \mathbf{k}_\alpha - \check{\mathbf{d}}[n-x]^H \mathbf{k}|^2 \right] \right] \quad (15)$$

Since both $\check{\mathbf{d}}[n]$ and $\check{\mathbf{d}}[n-x]$ contain per definition only uncorrelated variables, it is easy to prove that the optimal kernel in the sense of the MMSE criterion is given by

$$\check{\mathbf{k}}_\alpha^{(x)} = \mathbf{C} \mathbf{k}_\alpha \quad (16)$$

with

$$\mathbf{C} \triangleq \mathbb{E} \left[\check{\mathbf{d}}[n-x] \check{\mathbf{d}}[n]^H \right] \quad (17)$$

where $\mathbf{C} \in \{0, 1\}^{N_r \times N_r}$. The under-modeling error for this specific delay and output $\sigma_{u, \alpha}^2(x)$ equals

$$\begin{aligned} \sigma_{u, \alpha}^2(x) &\triangleq \mathbb{E} \left[\left(\check{\mathbf{d}}[n]^H \mathbf{k}_\alpha - \check{\mathbf{d}}[n-x]^H \check{\mathbf{k}}_\alpha^{(x)} \right)^2 \right] \\ &= \mathbf{k}_\alpha^H (\mathbf{I} - \mathbf{C}^H \mathbf{C}) \mathbf{k}_\alpha \end{aligned} \quad (18)$$

Using the previously obtained result, the MMSE delay m is selected using

$$[m] = \underset{x \in \{0, \dots, M\}}{\text{argmin}} \left[\sum_{\alpha=1}^L \sigma_{u, \alpha}^2(x) \right] \quad (19)$$

where the fact is used that an m greater than M can never be optimal.

As stated before, the RMDM does not completely describe the FDM, such that an equalizer deploying the RMDM will not exploit fully the information present in the RX signal. On the contrary, the unused part will have a noise-like effect from the equalizer's point of view. Hence, the noise variance at the α -th output of the RMDM,

$$\sigma_{\check{\eta}, \alpha}^2 = \sigma_{\eta, \alpha}^2 + \sigma_{u, \alpha}^2(m). \quad (20)$$

The noise signal $\check{\eta}[n, \alpha]$ is most likely no longer Gaussian nor white. Hence, a closed-form expression for the performance degradation due to the under-modeling is not easily

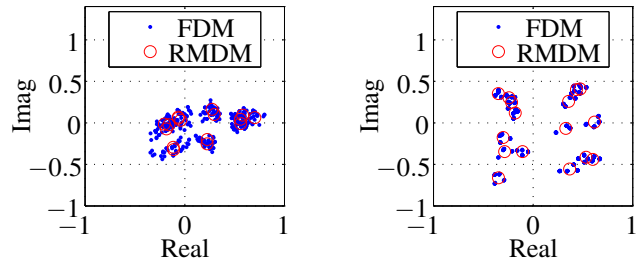


Figure 1: Constellation diagram at the outputs of a FDM and its RMDM. The left-hand plot refers to $\alpha = 1$ and the right-hand plot to $\alpha = 2$

obtained. An indication for the performance is obtained by computing the "overall SNR" seen from the equalizer's perspective, namely

$$SNR_{RMDM} = \sum_{\alpha=1}^L \frac{\|\check{\mathbf{k}}_\alpha\|^2}{\sigma_{\check{\eta}, \alpha}^2 + \sigma_{u, \alpha}^2(m)}. \quad (21)$$

The ability of an RMDM to mimic its FDM can be visualized by comparing their constellation diagrams. In Fig. 1, the constellation diagram is depicted of a memory-four FDM describing a QPSK-TR system, together with the constellation diagram of its memory-one RMDM. The RMDM's constellation diagram resembles the constellation diagram of the FDM reasonably well, in the sense that the general structure of the FDM's constellation is preserved. Using the RMDM, an equalizer is likely to decode the received signal correctly. The system will have an increased sensitivity to noise, but its equalizer complexity is reduced by a factor of 64.

4. SYSTEM DESCRIPTION

In this section, several QPSK-TR systems will be investigated with respect to performance and complexity. The general structure of the system, depicted in Fig. 2, is as follows. Information bits are encoded to channel bits using a turbo code. These channel bits are first passed through an interleaver Π and then fed into a de-multiplexer, to obtain N_{sb} parallel channel bit streams. Each bit stream is communicated over N_{sb} parallel channels, obtained by dividing the spectral resources into N_{sb} sub-bands. In each sub-band, QPSK-TR signaling will be applied and demodulated using a fractionally sampled AcR. Hence, the system is operating over N_{sb} parallel concatenated FDMs. Each FDM is equalized using a trellis-based equalizer, generating logarithmic-likelihood-values (LLVs) for the channel bits. The LLVs generated by the N_{sb} equalizers are multiplexed to a single LLV stream, de-interleaved and processed by an FEC decoder. The presence of a de-interleaver Π^{-1} ensures that little to no correlation exists between neighboring LLVs, such that the full potential of the FEC can be exploited.

Let us clarify the purpose of using sub-bands. With increasing data-rate, the channel memory will unavoidably increase, such that the equalizer complexity must be increased as well, to fully exploit the information present in the received signal. Unfortunately, its complexity grows exponentially with the channel memory, making it quickly too complex for any realistic application. To avoid too complex equalization, while still allowing for a high data-rates,

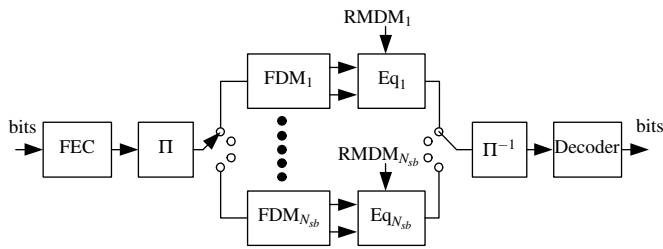


Figure 2: Model of the communication chain

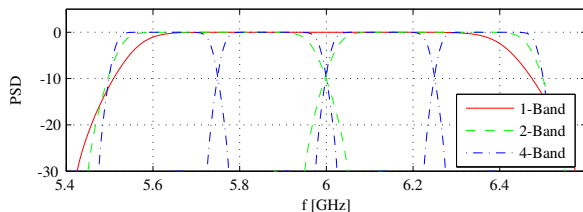


Figure 3: Division of the spectral resources into sub-bands

[2] proposed to divide the spectral resources into sub-bands. In each sub-band, the data-rate will be relatively low, such that the channel memory is relatively low. Our goal is a system providing a high data-rate with a limited amount of sub-bands—to avoid complex filter-banks—, while simultaneously limiting the equalizer complexity.

Three system architectures will be considered, using 1, 2 and 4 sub-band(s) respectively. All achieve the same channel data-rate of 200 Mb/s, while occupying 1 GHz bandwidth centered around 6 GHz. In each sub-band, QPSK-TR signaling will be applied. The delay D had a value of 5, 10 and 20 [ns] for a system with 1, 2 and 4 sub-band(s), respectively. In Fig. 3, the division of the spectral resources into sub-bands has been depicted.

The mapping of channel bits on $\tilde{b}[n]$ and $b[n]$ can be found in Tab. 1. The symbol-rate depends on the number of sub-bands. The received signal is demodulated using an AcR, which is fractionally sampled at rate two, meaning that two samples are taken per symbol. The sampling phase is not synchronized to the received signal.

As a trellis-based equalizer, we used a soft-input, soft-output Log-Map equalizer, even though it is approx. twice as complex as a Viterbi equalizer. It is inherently better suited to generate LLVs for the channel bits, allowing the FEC decoder to correct more errors. The complexity of the Log-Map equalizer is proportional to the number of state-transitions, i.e. proportional to N_s^N . Note that the non-linearity of the channel has no significant impact on the equalizer complexity. Only the metric computations become more complex. In

Table 1: Symbol mapping table

bits	$s[n]$	$\tilde{b}[n]$	$b[n]$
00	0	1	j
01	1	-1	$-j$
10	2	-1	-1
11	3	1	1

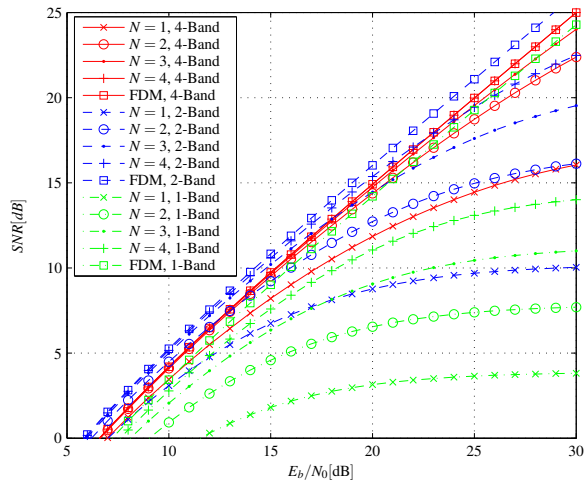


Figure 4: The average "overall SNR" of the RMDM as function of its memory

this work, the equalizers are assumed to have perfect information on the RMDMs, which are derived directly from the related FSMs. The memory of the RMDM has been varied from one to four, i.e. the number of states of the equalizer has been varied from 4 to 256.

All systems deploy the same rate-1/2 turbo code, such that the information bit-rate equals 100 Mb/s. The turbo code consists of two identical, parallel concatenated, rate-1/2, recursive systematic convolutional codes (RSCCs), defined by the polynomials (5, 7). The first RSCC receives the information bits directly, while the second RSCC encodes interleaved information bits. The interleaver block size equals 4098 information bits. Both coders are terminated. The turbo decoder conducts eight iterations for each information block.

The system performances are evaluated using a pool of NLOS channel realizations, measured at the IMST premises in an office of 4 by 4 by 2.5 meters [9]. These channels have an RMS delay spread of about 12 ns.

5. SIMULATION RESULTS

To get a feeling for the performance loss due to the sub-optimal equalizer, the SNR_{RMDM} , averaged over all channel realizations and sub-bands, has been depicted as a function of N in Fig. 4, for the three system models. Although the difference between the FDM SNR and the RMDM SNR can not be translated into the E_b/N_0 -loss in the BER-performance curves, it will give insight in the required equalizer complexity. Note that the E_b/N_0 -values depicted on the x-axis are with respect to the channel bits.

The figure shows that with an increasing number of sub-bands, the RMDM requires less memory to adequately mimic the FDM. In case of a system with four sub-bands, a 16-state RMDM (memory $N = 2$) is able to approximate the FDM for all channel realizations. Only at $E_b/N_0 > 20$ dB, a difference can be observed, which is well above the E_b/N_0 working point. In case of two sub-bands, a 64 states RMDM ($N = 3$) is at least required to adequately mimic the FDM for most channel realizations, while in the single band case, 256 states ($N = 4$) are by far not sufficient to mimic the FDM.

To validate the conclusions derived from Fig. 4, also the

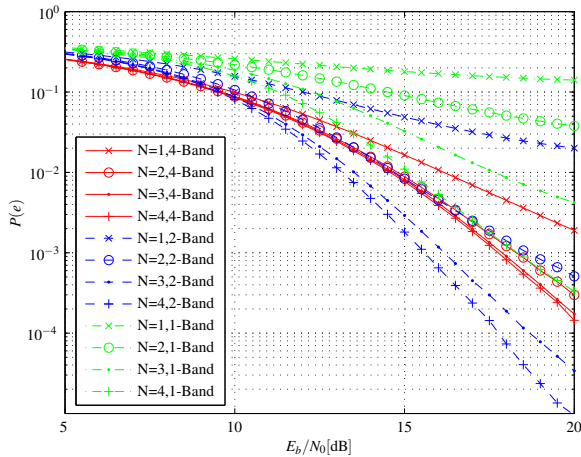


Figure 5: The average channel BER after the Log-Map equalizer of the three different systems

channel BER performance has been depicted as a function of E_b/N_0 for the three system architectures. To obtain insight on its effect on the performance, the equalizer complexity has been varied from 4 states to 256 states ($N = 1$ till 4).

In case of the four sub-band system, Fig. 5 confirms that 16-state equalization is sufficient. I.e. almost no further improvement is observed in the channel BER. In the two-band case, a similar result applies, but at least 64 states are needed to obtain close to optimal performance. In the single-band case, 256 states for the equalizer are not yet sufficient to extract the complete information available in the received signal. Additional gain seems possible.

The channel BER of the different system architectures can not be compared directly. The four-band system performs namely worse than the two-band system at high E_b/N_0 -values, since it does not exploit the complete frequency diversity available. It is the task of the FEC to exploit the remaining available frequency diversity. To illustrate this, the information BER has been depicted in Fig. 6. The figure shows that the FEC is indeed able to close the performance gap. In fact the four-band system performs slightly better than the two-band system—in terms of information BER—, even though its channel BER is considerable worse. Furthermore, it reveals that an E_b/N_0 of approx. 13 dB is needed to obtain virtually error-free communication, using the sub-optimal AcR.

6. CONCLUSIONS

A combination of trellis-based equalization and a multi-band system architecture has been investigated, to obtain high data-rate UWB communication over the multipath radio channel, using non-coherent receivers. To achieve this goal, a reduced-memory data model has been introduced for the non-linear sub-band channels. It is optimal in the sense of the MMSE criterion and allows for the study of the relationship between the equalizer complexity and the performance. Two multiband systems using two and four sub-bands achieved approx. the same performance after forward error control. The two-band system's RF-front-end is possibly less complex, at the cost of a more complex equalizer. A single-band system did not achieve the same performance for the limited

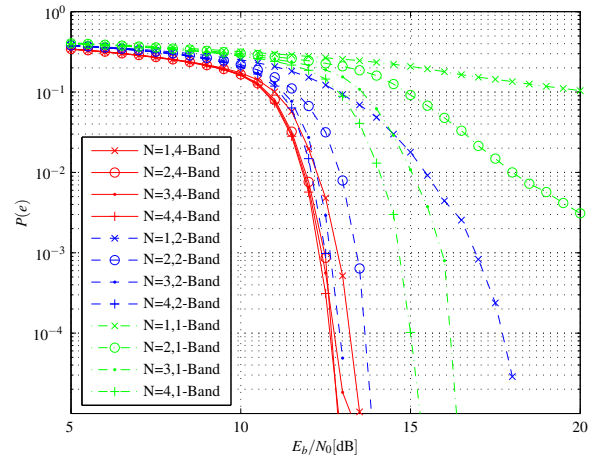


Figure 6: The average information BER after the Log-Map equalizer of the three different systems

amount of equalizer complexity invested in our simulations.

REFERENCES

- [1] M. Weisenhorn and W. Hirt, "Robust noncoherent receiver exploiting uwb channel properties," in *Intern. Works. UWB Syst. Joint with Conf. UWB Syst. and Techn., Joint UWBST & IWUWBS*, Kyoto, Japan, May 2004.
- [2] S. Paquelet, L.-M. Aubert, and B. Uguen, "An Impulse Radio asynchronous Transceiver for high data rates," in *Intern. Works. UWB Syst. Joint with Conf. UWB Syst. and Techn., Joint UWBST & IWUWBS*, 2004, pp. 1–5.
- [3] R. Hocht and H. Tomlinson, "Delay-hopped transmitted-reference RF communications," in *IEEE Conference on Ultra Wideband Systems and Technologies*, Baltimore, MD, May 2002, pp. 265–270.
- [4] M. Ho, V. Somayazulu, J. Foerster, and S. Roy, "A differential detector for an ultra-wideband communications system," in *IEEE Vehicular Technology Conference, VTC*, vol. 4, 2002, pp. 1896–1900 vol.4.
- [5] H. Zhang and D. Goeckel, "Generalized transmit-reference UWB systems," in *IEEE Conference on Ultra Wideband Systems and Technologies*, Reston, VA, Nov. 2003.
- [6] J. Romme and K. Witrisal, "Analysis of QPSK Transmitted-Reference Systems," in *IEEE International Conference on Ultra-Wideband, ICU*, 2005.
- [7] K. Witrisal, G. Leus, M. Pausini, and C. Krall, "Equivalent system model and equalization of frame-differential impulse radio UWB systems," *IEEE Journal on Selected Areas in Communications*, vol. 23, no. 9, Sept. 2005.
- [8] M. Sahin and H. Arslan, "Inter-symbol interference in high data rate uwb communications using energy detector receivers," in *Ultra-Wideband, 2005 IEEE International Conference on*, 2005, pp. 176–179.
- [9] J. Kunisch and J. Pamp, "Measurement results and modeling aspects for the UWB radio channel," in *IEEE Conference on Ultra Wideband Systems and Technologies*, Baltimore, MD, May 2002, pp. 19–23.